peratures as the maxima in the thermal conductivity, and indeed, only appear at all in the samples which are among the best conductors of heat.

## ACKNOWLEDGMENTS

---

# Selective Spin Excitation and Relaxation in Nuclear Quadrupole Resonance*

M. J. WEBER† AND E. L. HAHN
*Department of Physics, University of California, Berkeley, California*
(Received May 6, 1960)

Nuclear relaxation in a quadrupolar spin system has been investigated by selectively exciting nuclei into particular magnetic levels and observing the transient recovery of the spin system toward an equilibrium population distribution. Selective excitation is achieved by correlating the frequency and precessional behavior of nuclei in certain states with applied elliptically and linearly polarized, pulsed radio-frequency fields. A quantum-mechanical analysis is presented to describe the excitation of a quadrupolar spin system produced by a pulsed, elliptically polarized rf field. Using selective excitation techniques, several new modes of longitudinal relaxation are observed. Experiments using the chlorine quadrupole resonance in a single crystal of KClO₃ demonstrate how these new relaxation modes are used (1) to study dynamic spin-spin interactions and cross relaxation between overlapping resonance lines, and (2) to determine the individual $\Delta m = \pm 1$ and $\pm 2$ quadrupolar spin-lattice relaxation transition probabilities. A method is introduced by which the magnetic dipole-dipole contribution to the resonance linewidth can be determined independently of static quadrupole broadening, by observing the decay of the beat modulation of certain free-induction signals caused by precession in a small magnetic field. The measured magnetic linewidth of $Cl^{35}$ in KClO₃ is in good agreement with the value obtained from a second-moment calculation.

## I. INTRODUCTION

PULSED nuclear magnetic induction techniques[1,2] are a convenient means for study of the direct transient recovery of a spin system toward thermal equilibrium. Thermal equilibrium among the spins is established by spin-spin interactions, if a spin temperature can be defined; and also a spin-lattice thermal equilibrium is established if a lattice temperature can be defined. The present paper describes the application of transient resonance techniques to the study of nuclear spin relaxation in quadrupolar spin systems. By means of selectively exciting nuclei into particular magnetic substates, additional important information about spin-spin cross-relaxation effects, quadrupolar spin-

lattice relaxation, and pure magnetic line broadening can be obtained.

In solids having noncubic symmetry, the interaction between the nuclear electric quadrupole moment and the crystalline electric field gradient can establish a system of well-defined quadrupole energy levels.[3] In zero magnetic field these energy states exhibit a characteristic twofold Kramer's degeneracy of $\pm m$, where $m$ is the magnetic quantum number. Although spins in $+m$ and $-m$ states have the same energy, they precess in opposite directions about the electric field gradient as a result of the quadrupole coupling. Therefore, when a linearly polarized rf field is used to excite a quadrupole resonance, both oppositely rotating circularly polarized components of the field are active in inducing transitions. One circularly polarized component excites spins in $+m$ states while the other excites spins in $-m$ states. The action of the rf magnetic field leads to an observable linearly polarized magnetization, oscillating in the direction of the exciting

[1] E. L. Hahn, Phys. Rev. 80, 580 (1950).
[2] M. Bloom, E. L. Hahn, and B. Herzog, Phys. Rev. 97, 1699 (1955).
[3] T. P. Das and E. L. Hahn, *Nuclear Quadrupole Resonance Spectroscopy, Solid State Physics* (Academic Press, Inc., New York, 1958), Suppl. 1.

field, which arises from the superposition of two components, corresponding to spins in $+m$ and $-m$ states, rotating in opposite directions.[2]

The nuclear precessional properties of a quadrupolar spin system suggest a way of selectively exciting nuclei associated with a given frequency transition. If instead of a linearly polarized rf field, a circularly polarized rf field is applied, only one-half of the quadrupolar spin system will be excited, corresponding to nuclei in states of one sign of $m$ only.[4] When an elliptically polarized rf field is used, which can be decomposed into two oppositely rotating circularly polarized fields of different amplitudes, spins associated with transitions between $+m$ and $-m$ states will be excited differently. Thus the additional degree of freedom inherent in the rf field polarization enables one to divide a quadrupolar spin system into two separately observable subsystems composed of nuclei in $+m$ and $-m$ states.

Selective excitation using circularly polarized rf has the unique advantage that degenerate resonant transitions can be examined individually. Thus spin-spin interactions and cross relaxation can be studied between quadrupole resonance lines which are separated by arbitrarily small and variable Zeeman splittings. In general, whenever the $+m$ and $-m$ spin systems are selectively excited, several new modes of relaxation can be observed. Methods will be developed which illustrate how these new relaxation modes may be used to distinguish relaxation contributions from spin-lattice and spin-spin interactions, and, in addition, to determine the individual transition probabilities associated with $\Delta m = \pm 1$ and $\pm 2$ quantum number changes in quadrupole spin-lattice relaxation.

A quantum-mechanical analysis is presented in Sec. II which describes the excitation of a quadrupole spin system by an elliptically polarized pulsed rf field. The observed nuclear free magnetic induction signals following the rf pulse are calculated, and their properties are discussed for various rf field polarizations. From this analysis initial conditions are obtained which are inserted into the relaxation equations to be treated in Secs. III and IV. The theory of selective excitation and relaxation is verified by observation of the $Cl^{35}$ quadrupole resonance in $KClO_3$.

## II. SELECTIVE EXCITATION

### Elliptically Polarized rf

The general Hamiltonian for the excitation of the spin system is

$$\mathcal{3C} = -\mathbf{Q} \cdot \nabla \mathbf{E} - \gamma \hbar \mathbf{I} \cdot \mathbf{H}(t), \qquad (1)$$

where $\gamma$ is the gyromagnetic ratio and $\mathbf{H}(t)$ is the applied radio-frequency field. For the case of an axially symmetric electric field gradient tensor $\nabla \mathbf{E}$, the quadrupole interaction $\mathbf{Q} \cdot \nabla \mathbf{E}$ leads to the eigenvalue equation[3]

$$(\mathbf{Q} \cdot \nabla \mathbf{E}) \varphi_m = \frac{eqQ}{4I(2I-1)} [3m^2 - I(I+1)] \varphi_m = E_m \varphi_m, \quad (2)$$

where $q$ is the principal value of the field gradient at the nucleus, $Q$ is the nuclear quadrupole moment, and $I$ is the nuclear spin. The energy levels in (2) exhibit a characteristic $\pm m$ Kramer's degeneracy. In the case of spin $I = \frac{3}{2}$, which will be treated exclusively throughout this paper, there are two doubly degenerate energy levels giving rise to a single transition frequency at $\omega_0 = eqQ/2\hbar$.

Consider an elliptically polarized rf field $\mathbf{H}(t)$ applied to the spin system in a plane perpendicular to the field gradient symmetry axis, the $z$ axis of quantization. This field can be generated by two linearly polarized fields applied at right angles to one another with field amplitudes $H'$ and $H''$, respectively, angular frequencies $\omega$, and with a phase difference $\delta$:

$$\mathbf{H}(t) = \hat{x} H' \cos(\omega t) + \hat{y} H'' \cos(\omega t - \delta). \qquad (3)$$

The rf field is applied for a short pulse time $t_w$ which satisfies the condition $1/t_w \gg \gamma \Delta H$, where $\Delta H$ is the equivalent resonance linewidth in oersteds. This condition insures that the entire spin spectrum is excited. The spin system is assumed to be in thermal equilibrium with the lattice at time $t = 0$, prior to the application of the rf pulse during the interval $0 \leq t \leq t_w$. The total wave function $\psi$ for $I = \frac{3}{2}$ is written as an expansion in the orthogonal eigenfunctions $\varphi_m$ of the quadrupole Hamiltonian,

$$\psi = \sum_{m=-\frac{3}{2}}^{+\frac{3}{2}} C_m(t) \varphi_m \exp(-iE_m t/\hbar). \qquad (4)$$

By using (1) and (4) in the time-dependent Schrödinger equation and the resonance condition

$$\omega = \omega_0 = |E_{\pm\frac{3}{2}} - E_{\pm\frac{1}{2}}| \hbar^{-1},$$

a set of simultaneous differential equations is obtained for the time rate of change of the coefficients $C_m(t)$. The solutions for $C_m(t)$ are conveniently expressed in terms of the initial coefficients $C_m(0)$ by the matrix relation[3] $C(t) = RC(0)$, where

$$C(0) = \begin{pmatrix} C_{+\frac{3}{2}}(0) \\ C_{-\frac{3}{2}}(0) \\ C_{+\frac{1}{2}}(0) \\ C_{-\frac{1}{2}}(0) \end{pmatrix}. \qquad (5)$$

The transformation matrix $R$ is given by

$$R = \begin{bmatrix} \cos(\theta_+/2) & 0 & i\exp(i\alpha_+)\sin(\theta_+/2) & 0 \\ 0 & \cos(\theta_-/2) & 0 & i\exp(i\alpha_-)\sin(\theta_-/2) \\ i\exp(-i\alpha_+)\sin(\theta_+/2) & 0 & \cos(\theta_+/2) & 0 \\ 0 & i\exp(-i\alpha_-)\sin(\theta_-/2) & 0 & \cos(\theta_-/2) \end{bmatrix}, \qquad (6)$$

[4] M. J. Weber and E. L. Hahn, Bull. Am. Phys. Soc. 3, 324 (1959).

where $\theta_{\pm} = \sqrt{3}\gamma H_{\pm}t/2$, and

$$H_{\pm} = (H'^2 + H''^2 \pm 2H'H'' \sin\delta)^{\frac{1}{2}},$$

$$\alpha_{\pm} = \tan^{-1}\left(\frac{\mp H'' \cos\delta}{H' \pm H'' \sin\delta}\right). \quad (7)$$

$H_{\pm}$ and $\alpha_{\pm}$ are the magnitudes and phases, respectively, of the two circularly polarized rf fields, one rotating clockwise, the other counterclockwise, generated by the superposition of two linearly polarized alternating fields given by Eq. (3).

The expectation values of the components of nuclear magnetization during the period of free nuclear precession following the rf pulse are calculated using the solution of the Schrödinger equation for $t \geq t_w$ when $\mathbf{H}(t) = 0$. All nuclear spin relaxation effects are omitted. The results are

$$M_x = (\sqrt{3}N\gamma\hbar^2\omega_0/8kT)[\sin(\sqrt{3}\gamma H_+t_w/2) \sin(\omega_0 t - \alpha_+)$$
$$+ \sin(\sqrt{3}\gamma H_-t_w/2) \sin(\omega_0 t - \alpha_-)], \quad (8a)$$

$$M_y = (-\sqrt{3}N\gamma\hbar^2\omega_0/8kT)$$
$$\times [\sin(\sqrt{3}\gamma H_+t_w/2) \cos(\omega_0 t - \alpha_+)$$
$$- \sin(\sqrt{3}\gamma H_-t_w/2) \cos(\omega_0 t - \alpha_-)], \quad (8b)$$

$$M_z = (N\gamma\hbar^2\omega_0/8kT)[\cos(\sqrt{3}\gamma H_-t_w/2)$$
$$- \cos(\sqrt{3}\gamma H_+t_w/2)], \quad (8c)$$

where $N$ is the total number of spins.

The $M_x$ and $M_y$ components of magnetization can be looked upon as components of two macroscopic magnetization vectors, each of magnitude $\sqrt{3}N\gamma\hbar^2\omega_0/8kT$, given by $\mathbf{M}_+$ and $\mathbf{M}_-$, which precess, respectively, in the clockwise and counterclockwise directions. At thermal equilibrium it is convenient to consider these vectors as aligned, antiparallel to one another, along the $z$ axis of quantization for the system, realizing that the thermal magnetization differs from $\mathbf{M}_+$ and $\mathbf{M}_-$ by a factor $\sqrt{3}$, because the analysis does not yield strictly a classical model.[2] Since the $+m$ and $-m$ magnetization vectors arise from spins precessing in opposite directions, they are excited independently by one of the two circularly polarized components $H_{\pm}$ of the applied rf field. The angles $\theta_{\pm} = \sqrt{3}\gamma H_{\pm}t_w/2$ in (8) represent the angles through which $\mathbf{M}_+$ and $\mathbf{M}_-$ have been tipped toward the $xy$ plane by the rf pulse. The components of $\mathbf{M}_+$ and $\mathbf{M}_-$ in the $xy$ plane precess in opposite directions and therefore *add* in the $x$ direction and *subtract* in the $y$ direction as indicated by the $+$ and $-$ signs in (8a) and (8b). The decay of the precessing transverse components of magnetization has been omitted. Longitudinal relaxation of $M_z$ will be treated in detail in Sec. III.

The solutions in (8) are now examined for two rf field polarizations of special interest:

a. Linearly polarized rf: $H' = 2H_1$, $H'' = 0$. With

these conditions (8) reduces to

$$M_x = (\sqrt{3}N\gamma\hbar^2\omega_0/4kT) \sin(\sqrt{3}\gamma H_1t_w) \sin\omega_0 t,$$
$$M_y = M_z = 0. \quad (9)$$

Therefore in a quadrupole resonance experiment using a linearly polarized rf magnetic field, the observed free-induction signal is linearly polarized along the direction of the rf field. There is no signal perpendicular to this direction, and the sample always has zero net $M_z$ since spins in $\pm m$ states are excited equally.[2]

b. Circularly polarized rf: $H' = H'' = H_1$, $\delta = \pi/2$. For this case (8) reduces to

$$M_x = (\sqrt{3}N\gamma\hbar^2\omega_0/8kT) \sin(\sqrt{3}\gamma H_1t_w) \sin\omega_0 t,$$
$$M_y = (-\sqrt{3}N\gamma\hbar^2\omega_0/8kT) \sin(\sqrt{3}\gamma H_1t_w) \cos\omega_0 t, \quad (10)$$
$$M_z = (N\gamma\hbar^2\omega_0/8kT)[1 - \cos(\sqrt{3}\gamma H_1t_w)].$$

A circularly polarized rf field excites only one half of the quadrupole spin system corresponding to spins in states of one sign of $m$ only. The resulting free-induction signal is only one half as large as in (a), where all spins are excited, and the signal is circularly polarized and observable in any direction in the $xy$ plane. In addition, the sample now has a nonzero $M_z$ component of nuclear magnetization.

## Application of a Consecutive Double Pulse

The elliptically polarized rf field in a single pulse of the preceding section is the resultant of two linearly polarized fields applied simultaneously at right angles with a relative phase difference $\delta$. It is now shown that if the two fields are applied consecutively rather than simultaneously, a different net excitation of nuclei in $+m$ and $-m$ states is again obtained. Under certain conditions the final state of excitation of the quadrupolar spin system is identical to that obtained using circularly polarized rf. This double-pulse method of selectively exciting a quadrupolar spin system provides certain technical advantages which are discussed in Sec. VI.

An rf field pulse of time duration $t_{w1}$ is applied to a spin sample in the $x$ direction at time $t = 0$. At $t = t_{w1}$ another rf field from the same coherent source of duration $t_{w2}$ is applied at right angles to the first field but shifted in rf phase by an angle $\delta$. The Hamiltonian is given by (1) where now the rf magnetic field is described by

$$\mathbf{H}(t) = 2H_1 \cos(\omega_0 t)\hat{x}, \qquad 0 \leq t \leq t_{w1};$$
$$\mathbf{H}(t) = 2H_2 \cos(\omega_0 t - \delta)\hat{y}, \quad t_{w1} \leq t \leq t_{w1} + t_{w2}; \quad (11)$$
$$\mathbf{H}(t) = 0, \qquad t > t_{w1} + t_{w2}.$$

The pulse time widths $t_{w1}$ and $t_{w2}$ are assumed to be very short compared to the time required for individual nuclear spins to lose phase coherence.

The first rf pulse produces a transformation $C(t_{w1}) = R_1 C(0)$, where $R_1$ has the form of $R$ given by
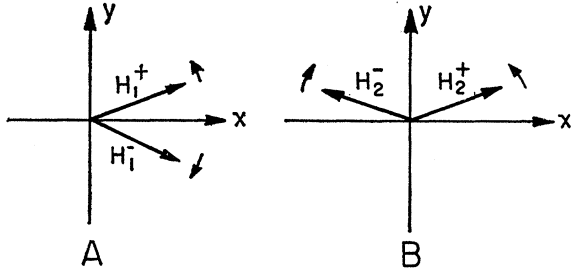
FIG. 1. Rf magnetic fields as seen by nuclei in $\pm m$ states during the two pulses used in the double-pulse technique. A. Oppositely rotating components of a linearly polarized rf field $H_1$ applied in the $x$ direction. B. Oppositely rotating components of a linearly polarized rf field $H_2$ applied in the $y$ direction and delayed in phase by $90°$ with respect to $H_1$.

Eq. (6) with $\theta_+ = \theta_- = \theta_1 = \sqrt{3}\gamma H_1 t_{w1}$ and $\alpha_+ = \alpha_- = 0$. The second pulse produces a further transformation described by $R_2$, with $\theta_+ = \theta_- = \theta_2 = \sqrt{3}\gamma H_2 t_{w2}$ and $\alpha_+ = \alpha_- = \delta$. The coefficients $C_m(t_w)$ at time $t_w = t_{w1} + t_{w2}$ are found from the combined transformation $C(t_w) = R_2 R_1 C(0)$. They are used in the solution of the Schrödinger equation after the double pulse to calculate the expectation values of the spin operators during the period of free precession. The associated macroscopic magnetization components for $t > t_w$ are

$$M_x = (\sqrt{3}N\gamma\hbar^2\omega_0/4kT)\,\sin(\sqrt{3}\gamma H_1 t_{w1})$$
$$\times [\cos^2(\sqrt{3}\gamma H_2 t_{w2}/2)\,\sin\omega_0 t + \sin^2(\sqrt{3}\gamma H_2 t_{w2}/2)$$
$$\times \sin(\omega_0 t + 2\delta)],$$

$$M_y = (-\sqrt{3}N\gamma\hbar^2\omega_0/4kT)\,\cos(\sqrt{3}\gamma H_1 t_{w1}) \qquad (12)$$
$$\times \sin(\sqrt{3}\gamma H_2 t_{w2})\,\sin(\omega_0 t + \delta),$$

$$M_z = (N\gamma\hbar^2\omega_0/4kT)\,\sin(\sqrt{3}\gamma H_1 t_{w1})$$
$$\times \sin(\sqrt{3}\gamma H_2 t_{w2})\,\sin\delta.$$

A classical picture of the excitation of a quadrupolar spin system by the double rf pulse is obtained by studying the behavior of the resultant magnetization vectors $\mathbf{M}_+$ and $\mathbf{M}_-$ subject to the rf magnetic fields shown in Fig. 1. During the first rf pulse the torques produced by $H_1^+$ and $H_1^-$ tip both $\mathbf{M}_+$ and $\mathbf{M}_-$ through an angle $\theta_1 = \sqrt{3}\gamma H_1 t_{w1}$. During the second pulse $\mathbf{M}_+$ is tipped through an additional angle $\theta_2 = \sqrt{3}\gamma H_2 t_{w2}$ by the field $H_2^+$. $\mathbf{M}_-$, however, sees a field $H_2^-$ directed oppositely to the field it experienced during the first pulse, and therefore is tipped back a negative angle $-\theta_2$. Thus the net effect of the double rf pulse is to nutate one sign of magnetization through an angle $(\theta_1 + \theta_2)$ while the other magnetization is nutated through an angle $(\theta_1 - \theta_2)$.

The solutions in (12) are now examined for the special case where the phase difference $\delta = 90°$ and the rf field-time product $H_1 t_{w1} = H_2 t_{w2}$. The latter condition makes the absolute nutations produced by the two pulses equal. Thus from the above discussion one sign of magnetization is nutated an angle $2\theta_1$ while the other will show no net effect after the double pulse. Under

these conditions Eqs. (12) reduce to results identical to those in (10) for a single pulse of circularly polarized rf capable of inducing a nutation angle $(2\sqrt{3}\gamma H_1 t_{w1})$.

When $\delta \neq 90°$ and $H_1 t_{w1} \neq H_2 t_{w2}$ the double rf pulse will still produce an unequal excitation of nuclei in $+m$ and $-m$ states. Equation (12) describes the resulting state of nuclear magnetization immediately after the two rf pulses. Although the magnetization vector picture of the excitation is possible, it is more complicated for the case where $\delta \neq 90°$ since the rotations $\theta_1$ and $\theta_2$ produced by the two rf pulses do not occur in the same plane. The visualization of the macroscopic behavior of the spin system is accordingly more complex. The effect of the first pulse is straightforward. The analysis of the second pulse is best made in the rotating frame of the magnetization vector of interest. It can be shown that the two rf pulses may be overlapped and the net excitation of the spins obtained will still be the same.

## Small External Magnetic Field

The effect of the application of a small magnetic field $H_0$ to the quadrupolar spin system, where $\gamma\hbar H_0 \ll eqQ$, is now considered. The addition of $H_0$ to the spin $\frac{3}{2}$ quadrupole system removes the $\pm m$ degeneracy and introduces a zero-order mixing of the $m = \pm\frac{1}{2}$ states.[5] The new set of eigenvalues and eigenfunctions for the system is given in Fig. 2. The applied rf field is again given by (3) and it is assumed that $t_w \ll 1/\gamma H_0$ and $H_1 \gg H_0$. The general expressions obtained for the expectation values of the spin operators following an rf pulse of elliptical polarization when $H_0 \neq 0$ are lengthy[6] and will not be given here. Instead consider the special case of an applied circularly polarized rf field where $H' = H'' = H$, and $\delta = \pi/2$. The $x$ component of precessing nuclear magnetization for $t \geq t_w$ is then given by[6]

$$M_x = \frac{\sqrt{3}N\gamma\hbar^2\omega_0}{8kT}\sin(\sqrt{3}\gamma H_1 t_w)$$

$$\times \left\{ \frac{f+1}{2f}\sin\left[\omega_0 + \Omega_0(\cos\theta_0)\left(\frac{3-f}{2}\right)\right]t \right.$$

$$\left. + \frac{f-1}{2f}\sin\left[\omega_0 + \Omega_0(\cos\theta_0)\left(\frac{3+f}{2}\right)\right]t \right\}, \quad (13)$$

where $\Omega_0 = \gamma H_0$, and $f = (1 + 4\tan^2\theta_0)^{\frac{1}{2}}$. A similar expression is obtained for $M_y$.

Since the circularly polarized rf pulse excites two lines $(\alpha', \beta')$ of the general four-line Zeeman spectrum for $I = \frac{3}{2}$, $M_x$ in (13) is made up of a superposition of two frequency components. The result is a modulation superimposed on the decay of the free-induction signals.

[5] C. Dean, Phys. Rev. 96, 1053 (1954).
[6] M. J. Weber, thesis, University of California (unpublished).

The phase of this modulation is the only difference between the expressions for $M_x$ and $M_y$. The remaining resonance lines $(\alpha,\beta)$ can be excited by circularly polarized rf of the opposite sense of rotation.

The $z$ component of nuclear magnetization following a circularly polarized rf pulse is given by

$$M_z = \frac{N\gamma\hbar^2\omega_0}{4kT} \sin^2(\sqrt{3}\gamma H_1 t_w/2)$$

$$\times \{1 + [(f^2-1)/2f^2][1-\cos(ft\Omega_0 \cos\theta_0)]\}. \quad (14)$$

Low-frequency terms proportional to the sine and cosine of the function $ft\Omega_0 \cos\theta_0$ have been omitted from $M_x$ in (13) since they produce a negligible induction signal in experiments where $\Omega_0 \ll \omega_0$. This low-frequency term, which has its origin in the magnetic-field mixing of the $m=\pm\frac{1}{2}$ states, is included in the expression for $M_z$, however, since it produces beats in free-induction signals to be discussed later. The magnetization along the quadrupole axis of quantization oscillates at the low Zeeman frequency. This results because another magnetization, made up of a superposition of spins in the mixed states, is actually precessing coherently about a different axis of quantization $z'$ determined by the angle $\theta$ which the applied field $H_0$ makes with respect to the $z$ axis.[7] The $z'$ axis lies in the plane of the $z$ quadrupole axis and $H_0$, at an angle $\theta'$ with respect to the $z$ axis, where

$$\theta' = \{2[(1+4\tan^2\theta)^{\frac{1}{2}}-1]/(1+4\tan^2\theta)\}^{\frac{1}{2}}.$$

An oscillatory population change of the mixed states is observed, analogous to the modulation of the intensity of light absorption in experiments on optical pumping when coherent spin precession occurs.[8]

Thus far only free-induction signals following a single rf pulse have been considered. If additional pulses are applied, quadrupole spin-echo signals[2] also occur. The calculation of spin-echo signals following excitation with circularly polarized rf is straightforward. The results are similar to those obtained by a linearly polarized field except for differences which enter because only one half of the spin system is excited;
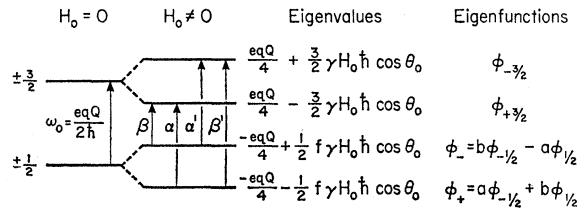


Fig. 2. Energy levels for spin $I=\frac{3}{2}$ axially symmetric quadrupole interaction perturbed by a small magnetic field $H_0$. A system of coordinates is chosen in which $\mathbf{H}_0 = H_0(\hat{x}\sin\theta_0 + \hat{z}\cos\theta_0)$. Parameters are $a=[(f-1)/2f]^{\frac{1}{2}}$, $b=[(f+1)/2f]^{\frac{1}{2}}$, $f=(1+4\tan^2\theta_0)^{\frac{1}{2}}$.

[7] M. Emshwiller, E. L. Hahn, and D. Kaplan, Phys. Rev. 118, 414 (1960).
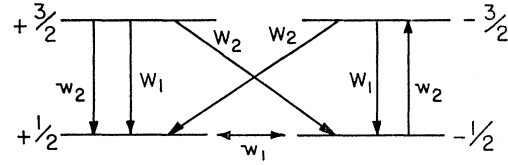[8] H. G. Dehmelt, Phys. Rev. 105, 1924 (1957).

Fig. 3. Relaxation transitions in a spin $\frac{3}{2}$ quadrupole system. Quadrupole spin-lattice relaxation transitions are labeled $W_1$ and $W_2$. $w_1$ and $w_2$ denote transitions arising from spin-spin interactions. The $w_2$ transitions represent the simultaneous flip of two spins.

namely (1) the echo amplitude is one-half as large, (2) the echo signal is circularly polarized, and (3) the echo modulation in a small magnetic field is different.

The double-pulse technique of selectively exciting spins is also applicable when a small magnetic field is present. The results and interpretation are similar to those obtained for excitation using elliptically polarized rf.

## III. LONGITUDINAL RELAXATION

Since the individual groups of $+m$ and $-m$ spin states may be excited and observed separately, the longitudinal relaxation or population changes of these separate spin subsystems can be studied rather than the relaxation of the total spin system. The energy levels for the $+m$ and $-m$ spin subsystems are shown in Fig. 3[9] for a spin $\frac{3}{2}$ system, together with allowed transitions leading to longitudinal relaxation of the $\pm m$ subsystems. In general, longitudinal relaxation of these two systems is determined by a combination of spin-lattice coupling and spin-spin coupling. $W_1$ and $W_2$ denote the transition probabilities per unit time for $\Delta m=\pm 1$ and $\pm 2$ quadrupolar spin-lattice relaxation. The transitions labeled by the probabilities per unit time $w_1$ and $w_2$ arise from secular magnetic dipole-dipole interactions involving the operators $I_\pm^i I_z^j$ and $I_\pm^i I_\pm^j$, respectively, of the dipolar interaction Hamiltonian[10] of spins $i$ and $j$.

The longitudinal relaxation is described by a set of simultaneous rate equations for the spin state populations $N_m$ of the form

$$\frac{dN_m}{dt} = \sum_n (W_{nm}N_n - W_{mn}N_m)$$

$$+ \sum_{k,l,n} (w_{lk,nm}N_lN_n - w_{kl,mn}N_kN_m). \quad (15)$$

The first summation describes the spin-lattice relaxation; the second summation is the additional relaxation contribution arising from spin-spin interactions. $w_{lk,nm}$ is the probability per unit time that a spin in state $l$ and a spin in state $n$ flip to new states $k$ and $m$, respectively.

[9] In an actual solid the degeneracy of the $\pm m$ levels is removed by local dipolar magnetic fields. The $\pm m$ label is used to refer to those states which become pure in the limit of zero magnetic field.
[10] N. Bloembergen, E. M. Purcell, and R. V. Pound, Phys. Rev. 71, 466 (1947).

A set of simultaneous rate equations (15) including the spin-lattice and spin-spin relaxation transitions shown in Fig. 3 are solved in the limit $eqQ/kT \ll 1$. The time dependence of the $z$-component macroscopic magnetizations $M^{\pm}(t)$ of the $\pm m$ subsystems following initial excitation at $t=0$, neglecting the short time $t_w$, is obtained as

$$M^{\pm}(t) = M_0 + A_1 \exp(\lambda_1 t) + A_2 \exp(\lambda_2 t) + A_3 \exp(\lambda_3 t), \quad (16)$$

where

$$\lambda_1 = -2(W_1 + W_2),$$
$$\lambda_{2,3} = -(W_1 + W_2 + w_1 + w_2) \pm [(W_1 - W_2 + w_2)^2 + w_1^2]^{\frac{1}{2}}. \quad (17)$$

The constants $A_{1,2,3}$ describing initial conditions are

$$A_1 = [M^+(0) + M^-(0) - 2M_0]/2,$$
$$A_2 = \left(\frac{a_-^2}{a_-^2 - a_+^2}\right)\left(\frac{M^+(0) - M^-(0)}{2}\right),$$
$$A_3 = \left(\frac{a_+^2}{a_-^2 - a_+^2}\right)\left(\frac{M^+(0) - M^-(0)}{2}\right), \quad (18)$$

where

$$a_{\pm} = \frac{W_1 - W_2 + w_2 - w_1 \pm [(W_1 - W_2 + w_2)^2 + w_1^2]^{\frac{1}{2}}}{W_1 - W_2 + w_2}, \quad (19)$$

and $M_0$ is the thermal equilibrium magnetization of the individual $+m$ and $-m$ subsystems.

The above results are obtained for a quadrupole system in zero external magnetic field. The spin-spin transition probabilities $w_1$ and $w_2$, however, are functions of both the magnitude and angle of any external magnetic field. If a small field $H_0$ is applied, the $\pm m$ degeneracy of the quadrupole energy levels is removed and the probability for spin-spin coupling is thereby reduced. At sufficiently large field strengths $(H_0 \gg \Delta H)$, the dipolar transition probabilities $w_1$ and $w_2$ become zero. In this limit $A_2 = 0$, $A_3 = [M^+(0) - M^-(0)]/2$, $\lambda_3 = -2W_1$, and (16) reduces to a linear combination of two exponential functions of the time. By measuring the decay constants of the two exponentials, the transition probabilities $W_1$ and $W_2$ for quadrupolar spin-lattice relaxation can be determined separately.

## IV. OBSERVATION OF LONGITUDINAL RELAXATION

The longitudinal relaxation of $M_z$ is observed by first applying a short intense pulse of rf to excite the spin system and reduce the equilibrium value of $M_z$. At some later time $\tau$ a second "inspection" pulse is applied to examine the relaxation of $M_z$ toward its equilibrium value. In pure quadrupole resonance using linearly polarized rf, the sum of the relaxation of the $\pm m$ subsystems is observed. From (16) this relaxation is described by

$$M^+(t) + M^-(t) = 2M_0 + [M^+(0) + M^-(0) - 2M_0] \times \exp[-2(W_1 + W_2)t], \quad (20)$$

and is due solely to spin-lattice coupling. The spin-lattice relaxation time $T_1$ is defined as

$$T_1 = 1/[2(W_1 + W_2)], \quad (21)$$

and is obtained directly by observing the "sum" signal of Eq. (20).

The use of linearly polarized rf in quadrupole resonance precludes the observation of the other terms in (16) which involve spin-spin interactions. The coefficients multiplying the second and third terms in (16) are proportional to $[M^+(0) - M^-(0)]$, which are zero when linearly polarized rf is used to excite the spin system initially because $M^+(0) = M^-(0)$. The terms of interest involving spin-spin coupling therefore vanish. The effects of spin-spin interactions can be studied by observing the individual relaxation of the $+m$ and $-m$ subsystems using circularly polarized rf excitation. However, since the transient recovery predicted by (16) is in the form of a linear combination of three exponential terms, the analysis of data and reduction to quantitative results would be difficult.

## Sum and Difference Signals

The independent measurement of (1) the rate at which internal spin-spin equilibrium among the $\pm m$ subsystems is established, and (2) the rate at which the total quadrupolar system attains thermal equilibrium with the lattice, can both be achieved by measurements derived from the relaxation of the "sum" and "difference" signals. Assume an elliptically polarized rf pulse is applied to excite a quadrupolar spin system. If a linearly polarized pulse is used to inspect the relaxation, the signal observed in the direction of the applied rf is the "sum" signal (20) described previously. If, however, the signal in the $xy$ plane perpendicular to the direction of the applied rf is observed, a "difference" signal corresponding to the amplitude difference of the two precessing $+m$ and $-m$ magnetizations is seen. The difference signal exists because, unlike the case of linearly polarized rf, elliptical rf polarization produces an unequal initial excitation of $\pm m$ spins. The amplitude of this signal is a measure of the magnetization difference of the $\pm m$ subsystems at the time the inspection pulse is applied.

The difference signal decays to zero as the spin system returns to internal equilibrium, and $M^+(t)$ and $M^-(t)$ approach equality. The form of this decay is obtained by subtracting $M^+(t)$ and $M^-(t)$ in (16), giving

$$M^+(t) - M^-(t) = 2A_2 \exp(\lambda_2 t) + 2A_3 \exp(\lambda_3 t), \quad (22)$$

where $\lambda_2$ and $\lambda_3$ are defined in (17) and include both spin-spin and spin-lattice interactions. Since spin-spin interactions have transition probabilities of order $1/T_2$, and generally $T_2 \ll T_1$ for solids, spin-spin coupling

between the $\pm m$ subsystems is the principal cause of the difference signal decay. This is particularly true at low temperatures where thermal spin-lattice processes are very slow.

The probability for spin-spin coupling between the $+m$ and the $-m$ spin systems can be varied and studied more thoroughly by introducing a small dc perturbing magnetic field. To interpret the resulting sum and difference signals, theoretical expressions are derived for these signals in the presence of a magnetic field.

Assume a spin $\frac{3}{2}$ quadrupole system is initially excited with a 180° circularly polarized rf pulse $R(180°)$. This pulse condition is chosen because (1) it maximizes the difference signal and, (2) there is no free-induction tail following the pulse which can interfere with the observation of the longitudinal relaxation immediately following the excitation pulse. The development of free precession following the pulse is described by a transformation operator $P(t)$. At time $t=\tau$ a 90° linearly polarized inspection pulse $R_i(90°)$ is applied in the $x$ direction. The expansion coefficients in $\psi$ after the second pulse are related to the initial ones by $C(\tau)=R_i(90°)P(\tau)R(180°)C(0)$. We assume the rf pulse widths are negligible compared to $\tau$. The $y$ component of precessing magnetization following the inspection pulse is

$$M_y = \frac{\sqrt{3}N\gamma\hbar^2\omega_0}{4kT}\cos\omega_0 t\left\{ b^4\cos\left[\Omega_0\cos\theta_0\left(\frac{3-f}{2}\right)t\right]\right.$$

$$+a^4\cos\left[\Omega_0\cos\theta_0\left(\frac{3+f}{2}\right)t\right]+2a^2b^2\cos(\tfrac{3}{2}\Omega_0\cos\theta_0 t)$$

$$\left.\times\cos\left[\frac{f}{2}\Omega_0\cos\theta_0(2\tau+t)\right]\right\}, \quad (23)$$

where $a$ and $b$ are defined in the caption of Fig. 2. A similar expression is obtained for $M_x$ which arises from magnetic precession of the $M_y$ signal.

Thus far no relaxation effects have been introduced into the calculation of (23). To include a rigorous treatment of longitudinal relaxation, the differential equations for the time rate of change of the diagonal elements $C_m{}^*C_m$ of the density matrix for the spin system must be solved. Here general expressions for $M_x$ and $M_y$ are derived by first calculating the free-induction signals in the absence of relaxation, and then introducing relaxation of $|C_m(t)|^2$ based on Eq. (15), using the free-induction values as initial conditions. The form of these solutions is in good agreement with the shape of the decays which are measured. Solutions are given for two special orientations of the magnetic field.

1. $\theta_0=0$.—With initial conditions $M^+(0)=-M_0$, $M^-(0)=M_0$, the transverse components of magneti-

zation following a 90° inspection pulse at $t=\tau$ are

$$M_x = 2M_0[1-\exp(\lambda_1\tau)]\cos\Omega_0 t\sin\omega_0 t$$
$$-[2M_0/(a_-{}^2-a_+{}^2)][a_-{}^2\exp(\lambda_2\tau)$$
$$-a_+{}^2\exp(\lambda_3\tau)]\sin\Omega_0 t\cos\omega_0 t;$$
$$M_y = 2M_0[1-\exp(\lambda_1\tau)]\sin\Omega_0 t\sin\omega_0 t \quad (24)$$
$$-[2M_0/(a_-{}^2-a_+{}^2)][a_-{}^2\exp(\lambda_2\tau)$$
$$-a_+{}^2\exp(\lambda_3\tau)]\cos\Omega_0 t\cos\omega_0 t.$$

Both the $M_x$ and $M_y$ signals contain a superposition of two relaxation processes: (1) the recovery of the total system toward thermal equilibrium behaving as $[1-\exp(\lambda_1 t)]$, and (2) the equilibration of the $\pm m$ subsystems behaving as $[a_-{}^2\exp(\lambda_2 t)-a_+{}^2\exp(\lambda_3 t)]$. Since the phase of the magnetic field sinusoidal modulation factor of the first and second terms in the expressions for $M_x$ and $M_y$ in (24) differ by 90°, the observation of either $M_x$ or $M_y$ as a function of pulse separation $\tau$ will be characterized by a decay to zero of the initial modulation peaks, while simultaneously the initial modulation nulls grow to become peaks at $t=\infty$. Measurement of the two relaxation phenomena is made by observing the decay and growth processes separately.

2. $\theta_0=90°$.—A similar calculation of the transverse magnetization components for this field orientation yields

$$M_x = 2M_0[1-\exp(\lambda_1\tau)]\cos\Omega_0 t\sin\omega_0 t,$$
$$M_y = [2M_0/(a_+{}^2-a_-{}^2)][a_-{}^2\exp(\lambda_2 t)+a_+{}^2\exp(\lambda_3 t)] \quad (25)$$
$$\times[\cos\Omega_0 t+\cos\Omega_0(2\tau+t)]\cos\omega_0 t.$$

When $\theta_0=90°$ there are no orthogonal signal components arising from magnetic precession and, therefore, the signals in (25) are not complicated by the superposition of two simultaneous relaxation phenomena. $M_x$ is a direct measure of the spin-lattice relaxation of the total system, while $M_y$ reveals the magnetization difference of the $\pm m$ subsystems.

## V. MEASUREMENT OF MAGNETIC LINE BROADENING

One of the modulation factors in (23) involves $\tau$, the pulse separation. This introduces a periodic amplitude variation of $M_z$ of period $\sim 2\pi/\Omega_0$ as $\tau$ is increased. The variation originates in the low-frequency term in the expression for $M_z$ in (14) arising from the magnetic field mixing of the $m=\pm\frac{1}{2}$ states. Although the oscillation of $M_z$ is not observed directly, the instantaneous value of $M_z$ at time $\tau$ is projected into the $xy$ plane by the 90° inspection pulse. The oscillation, therefore, appears as a periodic modulation of the over-all amplitude of the free-induction signal as a function of $\tau$. A similar beat modulation occurs in quadrupole spin echoes.[11]

Since there is always a spread in $H_0$, due either to external field inhomogeneities or to local magnetic

[11] M. Bloom, Phys. Rev. **94**, 1396 (1954).

dipole fields of nuclear neighbors, the above periodic modulation of the envelope of the difference signal amplitude will decay to zero in time. To include this decay, (23) must be multiplied by a distribution function describing the variation of $H_0$ and $\theta_0$, and integrated over all possible values. A Gaussian function of the form

$$g(\Omega-\Omega_0) = \exp[-(\Omega-\Omega_0)^2/2\varphi^2]/(2\pi\varphi^2)^{\frac{1}{2}} \quad (26)$$

is assumed to describe the distribution of $H_0$ due to neighboring spins. $\varphi$ is the root-mean-square deviation of the frequency due to the internal dipolar magnetic fields. The average of (23) over the distribution function (26) introduces a multiplicative factor

$$\exp[-\varphi^2 f^2(\cos^2\theta_0)(2\tau+t)^2/8]. \quad (27)$$

In general we must also average over the field angle $\theta_0$ since the angle for the internal dipolar field at different nuclear sites varies in direction. If, however, the externally applied field is much greater than local internal fields, the angle of the resultant field will equal approximately the angle of the external field. Thus we choose not to average over this angle and will assume $\varphi$ is equivalent to an internal field which lies along the direction of the externally applied $H_0$, independent of $\theta_0$.

The decay of free-precession signals is caused by spin-dephasing effects due to variations in both local electric field gradients and magnetic fields. The rate of decay of the modulation described above, however, depends only upon the magnetic field distribution. Therefore, this decay may be used to provide a measure of dipole broadening independent of electric field gradient broadening.[12] The broadening of the $Cl^{35}$ resonance in $KClO_3$ is measured in this fashion, and is discussed in Sec. VII.

## VI. APPARATUS AND TECHNIQUES

The nuclear quadrupole resonance spectrometer used to perform experiments utilizing all the techniques of selective excitation and observation described previously is shown in the block diagram, Fig. 4. The apparatus operates in the region of 30 Mc/sec. The rf source is an oscillator with an output gated into two rf channels, one of which contains a variable delay-line rf phase shifter. The input rf in the two channels is amplified, and the output is coupled into two orthogonal transmitting coils shown pictorially in Fig. 4. The inner solenoidal coil which holds the sample also functions as a pickup coil for the nuclear free-precession signal. This signal is amplified and detected in the receiver, and the final signal presentation is made on an oscilloscope. A signal integration circuit and an oscilloscope

---

[12] I. Solomon [Phys. Rev. **110**, 61 (1958)] has demonstrated how multiple spin echoes may be used to make the converse measurement, namely, the determination of the average of random quadrupole interactions independently of magnetic dipole-dipole broadening.

camera are used to measure and record simultaneously the relaxation of the nuclear induction signals.

The use of two rf gates permits versatility in carrying out measurements. Experiments requiring elliptically polarized rf are performed by opening the two rf gates simultaneously and adjusting the rf amplitude and phase difference of the two superimposed linearly polarized fields in order to obtain the desired resultant polarization. If the double-pulse technique of selective excitation is used, the rf gates are open consecutively. When only one rf gate is opened, experiments with linearly polarized rf are performed. Since free-induction signals are always observed with the inner solenoidal coil, the signals associated with the use of linearly polarized rf inspection pulses are observed either in the direction of the applied rf or perpendicular to it, depending upon whether the solenoidal or Helmholtz coil is pulsed. Therefore the "sum" signal is observed when the solenoidal coil is pulsed, and the "difference" signal is observed when the Helmholtz coil is pulsed.

Although both the elliptically polarized rf and double-pulse methods gave satisfactory results, most experiments requiring selective excitation of nuclei in $+m$ or $-m$ states were performed using the consecutive double-pulse technique, because the adjustment for the desired excitation was easier. In order to generate circularly polarized rf, the amplitude of the two superimposed rf fields must be equal, but to produce an equivalent excitation using the consecutive double-pulse technique, the rf field-time product $H_i t_{wi}$ for the two pulses must be equal. Thus in the latter case if the two rf field amplitudes $H_1$ and $H_2$ are not equal, the pulse durations $t_{w1}$ and $t_{w2}$ are easily adjusted to compensate for the difference and to satisfy the $H_i t_{wi}$ equality criterion. The amplitude of the free-precession signal following the initial excitation pulse and the difference signal are used to indicate the proper adjustment of the time widths and phase difference of the two rf pulses.

The two-coil rf output head shown in Fig. 4 consists of a Helmholtz coil of $\frac{3}{4}$-in. radius and an inner solenoidal coil of $\frac{5}{8}$ in. length and diameter. A 90° pulse for the $Cl^{35}$ resonance of 25 microseconds is produced by the Helmholtz rf coil. Coupling between the coils is eliminated to a large degree by adjusting the solenoidal coil for orthogonality with respect to the axis of the Helmholtz coil. The sample consisted of a
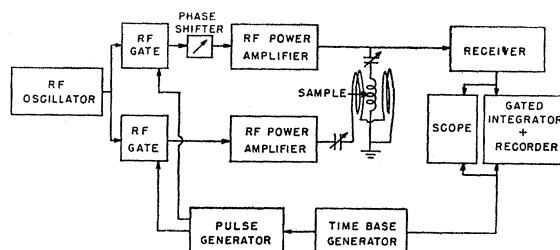


Fig. 4. Block diagram of apparatus.

single crystal, approximately cylindrical, with a length and diameter $\sim \frac{9}{16}$ in. The filling factor and homogeneity of the rf pulse fields with the above arrangement were satisfactory. The remaining components of the spectrometer are of standard design and similar to apparatus described elsewhere.[2,3]

## VII. EXPERIMENTAL RESULTS AND DISCUSSION

The theoretical predictions of selective excitation of nuclei in $+m$ and $-m$ states developed in II, and the analysis of the subsequent longitudinal relaxation in III and IV, have been verified by observation of the $Cl^{35}$ quadrupole free-precession signals in a single crystal of potassium chlorate.[13] This crystal is well suited for this investigation because the two $KClO_3$ molecules in the unit cell[14] have chemically and physically equivalent quadrupole resonance and Zeeman spectrum properties.

Using the spectrometer described in VI, both elliptically polarized rf and the double-pulse techniques were applied for selective excitation of nuclei in $+m$ and $-m$ states. The resulting free-induction signals confirmed the predictions of (8) and (12) with respect to their amplitude, polarization, and functional dependence on the rf polarization and field amplitudes.

A small magnetic field $H_0 \sim \Delta H$ was applied for the observation of the sum and difference signal relaxation. A series of photographs of the difference signal free-precession decay for various pulse separations is shown in Fig. 5 for a magnetic field orientation $\theta_0 = 0$. The sequence clearly illustrates the simultaneous decay of the Zeeman modulation peaks and the growth of the nulls of the $M_y$ signal as predicted by Eq. (24). The two separate relaxation rates are measured more conveniently by the use of a field orientation $\theta_0 = 90°$, since then only one relaxation process is present in the $M_x$ or $M_y$ signal expressed by Eq. (25).

FIG. 5. Series of photographs of oscillographic display of difference signal free-precession decay of $Cl^{35}$ in $KClO_3$ in a magnetic field $H_0 = 3$ oersteds applied at $\theta_0 = 0$. Photographs from top to bottom are taken at times $\tau = 0$, 10, 15, 25, and 100 milliseconds after the initial excitation pulse. Total sweep time is 2.0 msec. The initial spike is due to receiver recovery.
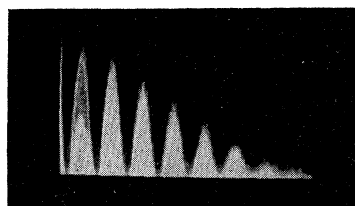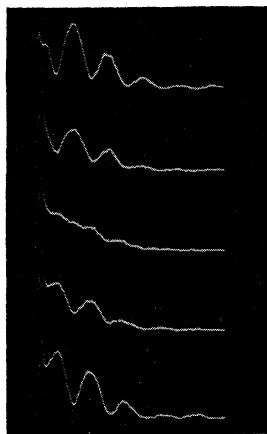
FIG. 6. Photograph of oscillographic display envelope trace showing amplitude modulation and relaxation of difference signal for $Cl^{35}$ in $KClO_3$. $H_0 = 2.7$ oersteds in the $\theta_0 = 90°$ direction. Total sweep time is 3.5 milliseconds.

The difference signal $M_y$ in Eq. (25) contains a sinusoidal amplitude modulation factor which is proportional to the time $\tau$ between excitation and inspection of the spin system. The envelope of this signal amplitude modulation is shown in Fig. 6 for a magnetic field at $\theta = 90°$. The general decay of the amplitude modulation peaks is due principally to spin-spin interactions which equilibrate the spin magnetizations of the $+m$ and $-m$ systems, thereby reducing the difference signal amplitude.

The contribution to the resonance linewidth arising from magnetic dipole-dipole interactions or external magnetic field inhomogeneities has been measured by utilizing the decay of the above modulation of the difference signal amplitude. Assuming a Gaussian decay factor given in Eq. (27), a root-mean-square local field at a chlorine site in $KClO_3$ of $(\langle \Delta H^2 \rangle)^{\frac{1}{2}} = 0.26 \pm 0.03$ oersted was found. To obtain consistent results independent of $H_0$, it was necessary to use a field $H_0 \gg \Delta H$, since then the neglect of the average over $\theta_0$ is less important. The broadening of quadrupole spectrum lines due to magnetic dipole-dipole interactions has been treated by Abragam and Kambe.[15] Applying their results to $KClO_3$, a moment of $(\langle \Delta H^2 \rangle)^{\frac{1}{2}} = 0.27$ oersted is obtained, which is in good agreement with the above measurement. This value of magnetic linewidth corresponds to a characteristic decay time $T_2^*$ of the free-precession signal which is more than twice as large as the observed value $T_2^* \sim 0.7$ millisecond. Thus quadrupolar line broadening was present in the crystal used in these experiments.

The dependence of the spin-spin interaction probabilities $w_1$ and $w_2$ upon magnetic field was investigated at room temperature by applying a small field $H_0$ to the sample at an angle $\theta_0 = 0$ to produce a Zeeman doublet of lines. Equation (22) predicts a time-dependent decay of the difference signal in the form of a linear combination of two exponential terms involving $w_1$ and $w_2$. As $H_0$ is increased, $w_1$, $w_2$, and the coefficient $A_2$ multiplying $\exp(\lambda_2 t)$ in (22) become smaller. In the limit $w_1$, $w_2 \ll W_1$, $W_2$, the coefficient $A_2$ approaches zero. The remaining simple exponential decay of the difference signal fits the data observed for fields $H_0 > 0.5$ oersted.

The $A_2 \exp(\lambda_2 t)$ term in (22) will always be less

[13] Dr. Ralph Livingston of the Oak Ridge National Laboratory kindly supplied the $KClO_3$ crystal used in these experiments.
[14] R. W. G. Wyckoff, Crystal Structures (Interscience Publishers, Inc., New York, 1957).

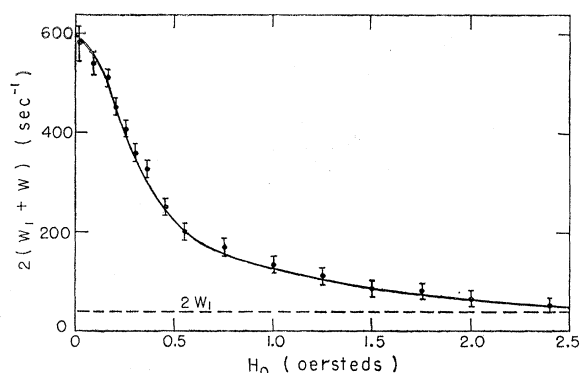[15] A. Abragam and K. Kambe, Phys. Rev. 91, 894 (1954).

FIG. 7. Characteristic relaxation rate of difference signal for $Cl^{35}$ in $KClO_3$ measured as a function of magnetic field $H_0$ applied in the $\theta_0=0$ direction.

important than $A_3 \exp(\lambda_3 t)$ since the multiplicative coefficient is smaller. However, for very small magnetic fields where $w_1$ and $w_2$ have their greatest value, this term should make a significant contribution to the relaxation process. In the region $0 < H_0 < 0.5$ oersted, due to inadequate cancellation of the earth's magnetic field and inhomogeneities over the sample, it was not possible to eliminate completely the amplitude modulation of the difference signal as a function of $\tau$. Thus the difference signal decay as a function of $\tau$ always had a sinusoidal modulation of long period superimposed upon it. This effect interfered with the accurate determination of the decay time dependence, and a decay proportional to a linear combination of two exponential terms could not be established. Therefore, all observations of the difference signal decay were fitted to a simple law of the form $\exp[-2(W_1+w)t]$. The measurements of the exponent $2(W_1+w)$ are plotted as a function of $H_0$ and are shown in Fig. 7.

The qualitative features of the data in Fig. 7 are as expected. In fields $H_0 < \Delta H$, spin-spin interactions are very probable, and the decay of the difference signal is due primarily to them, and is of order $1/T_2$. The decay rate decreases rapidly when $H_0$ becomes $\gtrsim \Delta H$, and the rate asymptotically approaches a limit $2W_1$, as predicted by (17) for $w_1=w_2=0$. The experiment may be viewed as the gradual separation of the two resonance lines associated with the circularly polarized resonance of the $+m$ and $-m$ states. Since spin-spin coupling between the lines is a function of the overlap of the two lines, the coupling is progressively decreased as $H_0$ is increased.

If we ascribe individual spin temperatures $T_s^{\pm}$ to the $+m$ and $-m$ spin systems, the above experiment may be interpreted thermodynamically as the thermal mixing of two systems of equal heat capacities. The two spin systems transfer heat to the thermal lattice both at a rate governed by the quadrupolar relaxation probabilities $W_1$ and $W_2$. Simultaneously the spins exchange energy between themselves at a rate determined by the spin-spin coupling quantity $w$. A treat-

ment using the spin-temperature concept[16] is confirmed by the observed exponential approach to temperature equilibrium between the two spin systems.

A theoretical calculation of the $H_0$ dependence of the spin-spin interaction probabilities involved in the difference signal decay is difficult. Certain hybrid methods combining perturbation methods and moment calculations of line shape have recently been attempted in a semiquantitative discussion of cross relaxation in spin systems.[17] In order to compute the transition probabilities using first-order perturbation theory, the density of the final states for a system of two overlapping interacting lines is required. As a first approximation one might treat pairs of spins whose mutual transitions conserve energy. We then consider a density function derived from $\int\int g_+(\omega_+)g_-(\omega_-)\delta(\omega_+-\omega_-)d\omega_+d\omega_-$, where $g_+$ and $g_-$ are the line shapes associated with the $+m$ and $-m$ spin systems and $\delta(\omega_+-\omega_-)$ is the delta function. Assuming a Gaussian line shape, this expression introduces a multiplicative factor $\exp(-H_0^2/\Delta H^2)$ into the first-order transition probability $w$, thereby predicting a Gaussian reduction of the different signal decay rate as $H_0$ is increased. The fitted curve in Fig. 7 is not Gaussian, however, but rather shows the presence of coupling when the $+m$ line and $-m$ line are separated by several linewidths—more than is predicted by the overlap of two Gaussian lines. Since accurate line-shape data was not available for the $Cl^{35}$ in our sample of $KClO_3$, the validity of the Gaussian line shape was not established; however, it is a reasonable first-order assumption for solids. The enchanced coupling when $H_0 > \Delta H$ may arise from higher order multiple-spin transitions. This type of process, although of higher order, utilizes the total frequency distribution of spins within the line and hence may be more important in providing coupling between lines at large separations.

The individual transition probabilities $W_1$ and $W_2$ for quadrupolar spin-lattice relaxation have been determined by applying a magnetic field of 75 gauss and selectively exciting and observing the relaxation of one of the Zeeman component lines shown in Fig. 2. If the magnetic field is applied at an angle $\theta_0=0$, the relaxation recovery of the $\alpha$, $\alpha'$ lines can be derived from (16) and is given by

$$M_{\alpha,\alpha'}(t)=M_0+A_1 \exp[-2(W_1+W_2)t]$$
$$\pm A_3 \exp(-2W_1 t), \quad (28)$$

where $w_1=w_2=0$. By combining observations of the relaxation of the total quadrupolar spin system given by (20) with that of (28), $W_1$ and $W_2$ are evaluated. Measurements at room temperature gave $T_1 = [2(W_1+W_2)]^{-1} = 21$ milliseconds, and $W_1 = 18.5$ $sec^{-1}$ and $W_2 = 5.4$ $sec^{-1}$ with an estimated error of $\pm 2$ $sec^{-1}$.

[16] R. T. Schumacher, Phys. Rev. 112, 837 (1958).
[17] N. Bloembergen, S. Shapiro, P. S. Pershan, and J. O. Artman, Phys. Rev. 114, 445 (1959).

This value of $W_1$ corresponds to the limiting value of $2(W_1+w)$ shown in Fig. 7 as the probability for spin-spin coupling approaches zero.

The ability to determine $W_1$ and $W_2$ is of considerable importance for the experimental verification of quadrupole spin-lattice relaxation theories. Since $W_1$ and $W_2$ are proportional to different components of the time-dependent electric field gradient tensor, the above measurement of $W_1 \sim 3W_2$ in $KClO_3$ reveals the relative importance of the $xz$ and $yz$, and $xx$, $yy$, and $xy$ tensor components of the field gradient. The separate measurement of $W_1$ and $W_2$ may be used to provide a sensitive and critical test of the theoretical model chosen to describe the source of the crystalline electric field gradient. A discussion of the measurements of $W_1$ and $W_2$ in $KClO_3$ and a comparison of the data with quadrupole spin-lattice relaxation theories will be considered in a separate paper.[18]
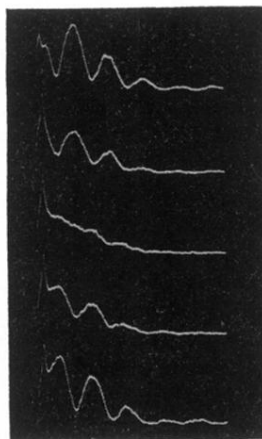
## VIII. CONCLUSION

The use of circularly polarized radiofrequency fields produces effects in a nuclear quadrupole spin ensemble which are similar to those obtained by the action of circularly polarized light in the method of optical pumping. By inducing spin transitions into excited states, so that a net change in spin momentum takes place, the degenerate states of the spin system become unequally populated, and the crystalline sample be-

comes macroscopically polarized. Following such a pulsed excitation, spin-spin and spin-lattice relaxation processes are observed as the spins repopulate the initial equilibrium states. Various components of relaxation can be distinguished from one another by adjustment of initial pulse excitation conditions and by variations of the magnitude and direction of small Zeeman fields relative to the crystalline axes. Given components of relaxation therefore are adjusted to become dominant, allowing them to be measured separately. The separate determination of spin-lattice relaxation due to $\Delta m = \pm 1$ and $\Delta m = \pm 2$ changes in spin momentum, previously unavailable, provides a critical test of current theories of nuclear quadrupole relaxation, and are discussed in detail in a separate paper. Spin-spin cross-relaxation effects can be measured for arbitrary separation of resonance lines by simply varying the magnitude of the Zeeman field. An absolute measurement of the pure magnetic dipolar broadening of the quadrupole coupled nucleus is demonstrated, which is not obscured by a spread in electric field gradient due to crystalline imperfections.

The selective excitation method is limited to the study of single crystals, where the simplest case of $Cl^{35}$, having one equivalent site in $KClO_3$, has been treated in this paper. Studies in crystals which contain more complicated nuclear quadrupole resonance spectra may also be made. However, the analysis of the experimental results would require a more involved extension of our present treatment.

[18] M. J. Weber, J. Phys. Chem. Solids (to be published).

Fig. 5. Series of photographs of oscillographic display of difference signal free-precession decay of $Cl^{35}$ in $KClO_3$ in a magnetic field $H_0=3$ oersteds applied at $\theta_0=0$. Photographs from top to bottom are taken at times $\tau=0$, 10, 15, 25, and 100 milliseconds after the initial excitation pulse. Total sweep time is 2.0 msec. The initial spike is due to receiver recovery.
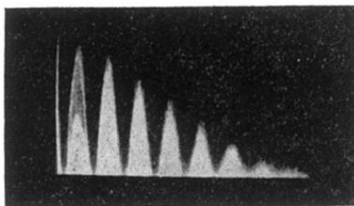
FIG. 6. Photograph of oscillographic display envelope trace showing amplitude modulation and relaxation of difference signal for $Cl^{35}$ in $KClO_3$. $H_0 = 2.7$ oersteds in the $\theta_0 = 90°$ direction. Total sweep time is 3.5 milliseconds.